Anionic Surfactant Templated Titanium Oxide Mesophase: Synthesis, Characterization, and Mechanism of Formation

Vittorio Luca,* Jonathan N. Watson, Martin Ruschena, and Robert B. Knott

Australian Nuclear Science and Technology Organisation, Institute of Materials and Engineering Sciences, PMB 1, Menai, NSW 2234, Australia

Received June 12, 2005. Revised Manuscript Received October 17, 2005

A novel synthetic method is described for the preparation of bulk titanium oxide mesophase (TOM) material with wormhole texture based on templating by inexpensive dodecyl sulfate surfactant. To contol hydrolysis and condensation reactions, a mixture of the Ti(III) salt of dodecyl sulfate and Ti(IV) isopropoxide are reacted in an alcohol solvent. Humidified air is passed over or through this solution eliminating alcohol by evaporation and introducing water. Under these controlled conditions, gelation takes place over a period of several days. The sulfated TOM compound produced using this method has limited thermal stability which precludes elimination of surfactant by calcination. However, anion exchange of the sulfate surfactant from the TOM can be easily accomplished using dilute solutions of oxo-anions such as molybdate, tungstate, and vanadate, and this makes pore space available under mild conditions. Progressive filling of the pores produces micro- to mesoporous multicomponent oxides that are stable to temperatures in the range 300−400 °C. The TOM wormhole materials show a single low-angle X-ray diffraction peak and have type IV nitrogen adsorption isotherms with little or no hysteresis once the surfactant is eliminated by ion exchange. The titanium oxide framework of the TOM material has an unusual structure that is elucidated using extended X-ray absorption fine structure analysis. Both short and long Ti−O bonds are observed in the TOM material that are not characteristic of bulk of nanocrystalline titania. Variable exchange of oxo-anion species potentially offers a level of pore size control through adjustment of the thickness of the second oxide layer as well as affording materials that are potentially useful in catalytic and photocatalytic applications. The formation mechanism of the TOM materials has been subjected to detailed study using in situ small-angle X-ray and neutron scattering techniques which show that spherical micelles begin to develop in the alcoholic precursor solution after about 2 h of reaction. These spherical micelles grow in diameter, and after about 11 h of reaction a transformation to cylindrical micelles occurs.

Introduction

Since the initial discovery of surfactant templating by Japanese[1] and American scientists,[2] most studies have been directed at the chemistry of silicate materials. While silicate mesoporous materials are generally simpler to prepare than are transition metal oxides as a result of the lower reactivity of the molecular precursors involved, they are insulators and are, therefore, generally less useful. Perhaps one of the potentially most useful transition metal oxide semiconductors is titanium oxide. It has numerous potential applications including in catalysis[3] and photocatalysis,[4] as photovoltaics,[5] as antireflective coatings, and as a battery electrode material.[6]

Our initial attempts in 1995 to produce first-row group IVB and VB transition metal oxide mesophases[7] addressed the use of nonaqueous solvents and the controlled addition of HCl to control hydrolysis and subsequent condensation reactions of oligomeric anionic vanadate species in solution which interacted electrostatically with simple (single chain) cationic surfactant molecules (CTAC). We stated at the time that "This careful addition of HCl to the nonaqueous medium perhaps serves to better control what might otherwise be a cascade of runaway polymerization/condensation reactions. We surmise that increased connectivity of vanadium polyhedra occurs at the micelle interface and that the eventual condensation of vanadium-coated micelles leads to a wall structure resembling vanadium pentoxide". In a subsequent study we went on to explore the details of vanadium solution chemistry using liquid-state V-51 NMR and were able to identify the building blocks involved in the vanadium oxide mesophase assembly.[8] Apart from limiting the availability of arguably the most important reactant in sol−gel chemistry through the use of initially nonaqueous solvents, an additional strategy involves the use of less reactive molecular precursors. Thus, a metal alkoxide $Ti(OR)_4$ where R is a larger alkyl group will in general be less reactive than one where the R group is smaller. Yet another strategy in the case of a transition metal oxide is to reduce the oxidation state of the metal center, that is, use Ti(III) instead of Ti(IV). The present

* To whom correspondence should be addressed. E-mail: vlu@ansto.gov.au. Tel.: 61-2-9717 3087. Fax: 61-2-9543 7179.

(1) Yanagisawa, T.; Shimizu, T.; Kuroda, K.; Kato, C. *Bull. Chem. Soc. Jpn.* **1990**, *63*, 988.
(2) Kresge, C. T.; Leonowicz, M. E.; Roth, W. J.; Vartuli, J. C.; Beck, J. S. *Nature* **1992**, *359*, 710.
(3) Vedrine, J. C., Ed.; 2000; p 145.
(4) Anpo, M. *Pure Appl. Chem.* **2000**, *72*, 1265.
(5) O'Regan, B.; Grätzel, M. *Nature* **1991**, *353*, 737.
(6) Macklin, W. J.; Neat, R. J. *Solid State Ionics* **1992**, *53*−*56*, 694.
(7) Luca, V.; MacLachlan, D. J.; Hook, J. M.; Withers, R. *Chem. Mater.* **1995**, *7*, 2222.
(8) Luca, V.; Hook, J. M. *Chem. Mater.* **1997**, *9*, 2731.

10.1021/cm051255k CCC: $33.50 Published 2006 by the American Chemical Society
Published on Web 01/31/2006

study describes our efforts at deploying a combination of these strategies to prepare from one of the simplest surfactants of all (dodecyl sulfate) titanium oxide mesophase (TOM) materials with wormhole texture and interesting surface properties.[9]

Early attempts to prepare mesoporous titanium oxides started with the work of Antonelli and Ying using simple phosphate esters.[10] While claims of ordered materials were based mainly on transmission electron microscopy (TEM) images of uncalcined materials, calcined materials had poorly defined X-ray diffraction (XRD) patterns and type IV adsorption isotherms with large hysteresis loops which are generally indicative of a bottleneck or, in other words, a partially collapsed pore structure.[11] The materials prepared using these synthesis strategies were later shown to be mostly lamellar.[12] Phosphate surfactant systems also suffer the drawback that it is virtually impossible to remove the phosphate, and, therefore, semiconductor and photocatalytic properties are lost.[13]

Stucky and co-workers[14] were the first to report the preparation of bulk ordered TOMs using block copolymers (BCs; BASF, Pluronic P123). In their preparation, $TiCl_4$ was added to an ethanolic solution of P123 in the ratio 1:21.7:0.02 $TiCl_4$/EtOH/P123. The resulting solution was allowed to gel in an open container in ambient air at unspecified relative humidity (RH) and temperature. Again, while discrete regimes of order could certainly be observed by TEM, the so-produced calcined bulk materials were characterized by poorly defined XRD patterns and type IV adsorption isotherms with large hysteresis loops characteristic of blocked or bottleneck pores. In more-or-less a restatement of our earlier assertions, they went on to comment that "Restrained hydrolysis and condensation of the inorganic species appears to be important for forming mesophases of most of the non-silica oxides, because of their strong tendency to precipitate and crystallize into bulk oxide phases directly in aqueous media".

In a modification of this initial preparative procedure the Sanchez group[15−19] has published extensively on the preparation and characterization of highly ordered titanium oxide thin films also using BC systems and similar metal/surfactant ratios. However, by introducing water during the preparation of the highly acidic reactant solutions followed by controlled evaporation, the so-called evaporation induced self-assembly (EISA) paradigm,[20] they were able to promote initial hydrolysis to form discrete titanate clusters which then allow condensation to proceed in a controlled manner. This culminates in the first instance with a green gel, or the so-called moldable steady state, in which condensation is incomplete requiring mild thermal treatment of the composite material for stabilization.[21]

As compared to thin film samples made using BCs, highly ordered bulk TOMs obtained from simple surfactants (single chain surfactants with monofunctional headgroup) without any postsynthetic treatment are hard to come by. Many reports describe the use of neutral amine surfactants to produce bulk titanate mesophases with mostly wormhole structures and in some cases good thermal stability obtained by postsynthetic treatment.[22] There have been relatively few reports of the exploitation of ionic surfactants. Soler-Illia et al.[23] describe the production of bulk hexagonal and wormlike materials using the simple cationic surfactant cetyltrimethylammonium bromide (CTAB) and the EISA paradigm, but these materials do not match the order exhibited by films made using BCs. On[24] has also described products made using quarternary ammonium surfactants that initially are lamellar but can then be converted to poorly ordered hexagonal structures on postsynthetic treatment with NaOH.

One report by Nagamine and Sasaoka[25] describes the use of anionic surfactants (sodium dodecyl sulfate, SDS) and titanium tetraisopropoxide, which were reacted under acidic conditions to yield ostensibly lamellar products. It is the extremely low cost of this precursor that makes it particularly worthy of more detailed investigation for the preparation of bulk materials. In addition, the ability to remove sulfate is likely to be much more straightforward than the removal of phosphate. Indeed, other nontitanate mesostructured oxides have also been synthesized recently using this surfactant,[26−29] confirming that the sulfate esters can be more easily removed than their phosphate counterparts at least in these systems. There is good reason to believe, therefore, that it should be possible to remove sulfate from a titanate mesophase also. In this contribution we examine the possibility that mesoporous titanate materials can be synthesized using dodecyl sulfate and explore avenues for its facile removal once the titanate network has formed.

In comparison to most high valent transition metal ions which form mostly large anionic oligomeric species at

(9) Luca, V. WO Patent 0236494, 2002.
(10) Antonelli, D. M.; Ying, J. Y. *Angew. Chem., Int. Ed. Engl.* **1995**, *34*, 2014.
(11) Van Der Voort, P.; Ravikovitch, P. I.; De Jong, K. P.; Neimark, A. V.; Janssen, A. H.; Benjelloun, M.; Van Bavel, E.; Cool, P.; Weckhuysen, B. M.; Vansant, E. F. *Chem. Commun.* **2002**, 1010.
(12) Putnam, R. L.; Nakagawa, N.; McGrath, K. M.; Yao, N.; Aksay, I. A.; Gruner, S. M.; Navrotsky, A. *Chem. Mater.* **1997**, *9*, 2690.
(13) Stone, V. F., Jr.; Davis, R. J. *Chem. Mater.* **1998**, *10*, 1468.
(14) Yang, P.; Zhao, D.; Margolese, D. I.; Chmelka, B. F.; Stucky, G. D. *Nature* **1998**, *396*, 152.
(15) Crepaldi, E. L.; de Soler-Illia, G. J.; Grosso, D.; Cagnol, F.; Ribot, F.; Sanchez, C. *J. Am. Chem. Soc.* **2003**, *125*, 9770.
(16) Crepaldi, E. L.; Soler-Illia, G. J. de A. A.; Grosso, D.; Albouy, P.-A.; Amenitsch, H.; Sanchez, C. *Stud. Surf. Sci. Catal.* **2002**, *141*, 235.
(17) Grosso, D.; Soler-Illia, G. J. de A. A.; Crepaldi, E. L.; Cagnol, F.; Sinturel, C.; Bourgeois, A.; Brunet-Bruneau, A.; Amenitsch, H.; Albouy, P. A.; Sanchez, C. *Chem. Mater.* **2003**, *15*, 4562.
(18) Grosso, D.; Soler-Illia, G. J. de A. A.; Babonneau, F.; Sanchez, C.; Albouy, P.-A.; Brunet-Bruneau, A.; Balkenende, A. R. *Adv. Mater.* **2001**, *13*, 1085.
(19) Kallala, M.; Sanchez, C.; Cabane, B. *Phys. Rev. E: Stat. Phys., Plasmas, Fluids, Relat. Interdiscip. Top.* **1993**, *48*, 3692.
(20) Brinker, C. J.; Lu, Y.; Sellinger, A.; Fan, H. *Adv. Mater.* **1999**, *11*, 579.
(21) Grosso, D.; Cagnol, F.; Soler-Illia, G. J. de A. A.; Crepaldi, E. L.; Amenitsch, H.; Brunet-Bruneau, A.; Bourgeois, A.; Sanchez, C. *Adv. Funct. Mater.* **2004**, *14*, 309.
(22) Yoshitake, H.; Sugihara, T.; Tatsumi, T. *Chem. Mater.* **2002**, *14*, 1023.
(23) Soler-Illia, G. J. de A. A.; Louis, A.; Sanchez, C. *Chem. Mater.* **2002**, *14*, 750.
(24) On, D. T. *Langmuir* **1999**, *15*, 8561.
(25) Nagamine, S.; Sasaoka, E. *J. Porous Mater.* **2002**, *9*, 167.
(26) Yada, M.; Machida, M.; Kijima, T. *Chem. Commun.* **1996**, 769.
(27) Yada, M.; Ohya, M.; Machida, M.; Kijima, T. *Chem. Commun.* **1998**, 1941.
(28) Yada, M.; Ohya, M.; Ohe, K.; Machida, M.; Kijima, T. *Langmuir* **2000**, *16*, 1535.
(29) Yada, M.; Kitamura, H.; Machida, M.; Kijima, T. *Inorg. Chem.* **1998**, *37*, 6470.

specific pH values and concentrations, the hydrolytic chemistry of Ti^{4+} is more limited. In the absence of complexing ligands, highly acidic titanium-containing solutions contain very small cationic molecular species. To initiate an electrostatic interaction with an ionic surfactant, the surfactant headgroup should be anionic. In solutions that contain complexing ligands such as alkoxides a coordinating anionic surfactant headgroup also has the potential to interact strongly with a metal center by displacing the alkoxide ligands. In either case, it should be possible using an anionic surfactant such as dodecyl sulfate to couple to either small cationic titanium species via an electrostatic interaction or to neutral alkoxy titanate clusters via ligand substitution. Having established such an interaction it would then be possible induce hydrolysis and condensation in a controlled way to form a titanate framework in the presence of surfactant.[9]

In the present contribution we employ a strategy that is similar to that used by us to make mesostructured vanadium oxide using cetyltrimethylammonium surfactants[7,8] and which we subsequently patented.[9] The Ti(III) salt of the surfactant is first prepared, and this is then dissolved in ethanol. As previously stated the use of a Ti(III) surfactant salt helps to reduce hydrolysis rates because Ti(III) is less reactive toward hydrolysis than Ti(IV). Titanium isopropoxide is added to adjust the titanium-to-dodecyl sulfate ratio. This reactant solution is then exposed to a flux of humidified air to force the evaporation of alcohol and the simultaneous ingress of water.

The aims of the present work are (1) to explore routes to the preparation of titanate mesophase materials from simple and inexpensive surfactants, (2) to elucidate the nature of the phases that form, especially as far as the interface between the surfactant headgroup and the titanate component is concerned, and (3) to shed some light on the transformations that occur in solution during the hydrolysis and condensation using small-angle X-ray scattering (SAXS) and small-angle neutron scattering (SANS) techniques.

Experimental Section

Synthesis. A typical synthesis was accomplished in two stages. First the Ti(III)−dodecyl sulfate (TDS) was synthesized by adding 13.6 mL of a solution of 1.9 mol/L $TiCl_3$ in 2.0 mol/L HCl to 136 mL of an aqueous solution of SDS (Sigma; 200 g/L) such that the molar ratio of dodecyl sulfate to Ti was 3:1. This gave rise to the immediate precipitation of a lilac-colored solid which was separated by centrifugation. The solid was then washed twice by shaking with Milli-Q water, followed by centrifugation. Finally, the solid was freeze-dried and then stored in a nitrogen-filled glovebox. The freeze-dried product typically contained about 2.5 wt % water as shown by thermal analysis, and the chemical composition obtained was $(C_{12}H_{25}SO_4)_{3.0}Ti$ after extraction of the water component. Thus, the dodecyl sulfate/Ti ratio of the precursor remained 3. In the second step, the TDS salt precursor (5.0 g) was dissolved in 65 g of dry ethanol (Aldrich) to achieve an EtOH/Ti mole ratio of about 240 with warming to 60 °C. To this ethanolic solution was added titanium isopropoxide to adjust the Ti/dodecyl sulfate ratio to between 1 and 3. The final acidic ethanolic solution was a deep burgundy color. Within 2 h of exposure of this solution to still or flowing air the color changes from the initial deep burgundy to pale yellow. If this solution is isolated and further hydrolyzing is prevented, a crystalline eight-titanium atom oxo-alkoxysulfate cluster compound (Ti_8) can be isolated after a period of several months. If, however, air flow is continued so as to promote hydrolysis and condensation reactions, a glassy mesophase gel product (TOM) is formed. The formation of glassy TOM materials was carried out in a reproducible manner by employing a jacketed glass reactor in which a constant temperature (27−35 °C), a relative humidity (RH) of 80%, and an air flow of about 300 ± 50 mL/min were maintained. However, it was noted that some variation in temperature, RH, and air flow could be tolerated to also yield comparable materials. The pale yellow glassy gel TOM materials that were produced after reaction times exceeding 48 h were dried overnight in a 70 °C oven and in some cases heated in air at various temperatures for periods between 1 and 2 h. Ion exchange with simple tetrahedral oxo-anions such as $H_xVO_4^{2-x}$ and $H_xMoO_4^{2-x}$ was achieved by adding a calculated amount of a 40 mmol/L solution of the appropriate metal salt to a dispersion of the TOM in water followed by stirring for 30 min and separating the solid by centrifugation.

X-ray Absorption. X-ray absorption data were recorded in transmission mode on beamline 20B at the Photon Factory, Tsukuba, Japan, using a Si(111) double monochromator and narrow entrance and exit slits. Harmonics were eliminated by detuning of the monochromator. Analysis of the extended X-ray absorption fine structure (EXAFS) was performed with the programs XFIT[30] and FEFFIT.[31] To avoid thickness effects, samples were diluted and thoroughly mixed with boron nitride. To fit the EXAFS spectra, the values of the single E0 (the energy zero) and S_0^2, the so-called amplitude reduction factor, were obtained by fitting the EXAFS of the crystalline anatase reference sample with N (coordination number), R (distance in angstroms), and σ^2 (mean square relative displacement) initially fixed at their expected crystallographic values for titania and allowing E0 and S_0^2 to float simultaneously. The obtained values of E0 and S_0^2 were then used as the initial values for the nonlinear least-squares fit of the TOM samples. After optimization of N, R, and σ^2, E0 was allowed to float with the other parameters and usually settled close to the initial value.

XRD patterns were recorded on a Scintag X1 diffractometer using Cu Kα radiation. This instrument utilizes a Peltier detector with very low background. IR spectra were obtained using a Digilab FTS-40 spectrometer, equipped with a liquid-N_2-cooled mercury cadmium telluride detector. Samples (∼2 mg) were ground with KBr (200 mg) and pressed into disks. Nitrogen adsorption/desorption isotherms were obtained at 77 K on a Micromeritics ASAP 2400.

SAXS. In situ SAXS measurements were performed at the Research School of Chemistry at the Australian National University using the SAXS camera which has been described in detail elsewhere.[32] With a specially designed apparatus (Figure 1) in which temperature, ambient humidity, and air flow rate could be controlled, in situ measurements of the scattering functions were undertaken as the hydrolysis condensation reactions proceeded. The temperature, RH, and air flow rates used were those used to prepare the bulk materials. Data were taken at 1 h intervals over a 48 h period.

SANS: Contrast Variation Study. The intensity $I(Q)$ of the small-angle scattering from a solid particle depends on the difference in scattering length density (SLD) between the solute, ρ_m, and solvent, ρ_s, phases ($\rho_m - \rho_s$), as has been shown.[33] Isotopic

(30) Ellis, P. J.; Freeman, H. C. *J. Synchrotron Radiat.* **1995**, *2*, 190.
(31) Stern, E. A.; Newville, M.; Ravel, B.; Yacoby, Y.; Haskel, D. *Phys. B: Condens. Matter* **1995**, *208*−*209*, 117.
(32) Aldissi, M.; Henderson, S. J.; White, J. W.; Zemb, T. *Mater. Sci. Forum* **1988**, *27*−*28*, 437.
(33) Jacrot, B. *Rep. Prog. Phys.* **1976**, *39*, 911.

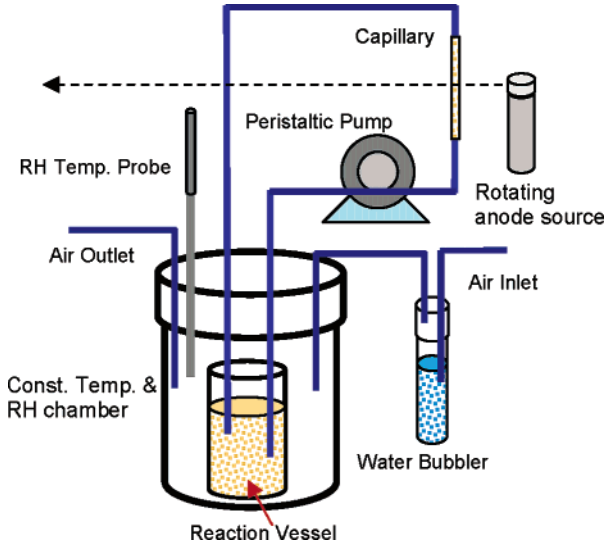

Figure 1. Setup used for in situ SAXS experiments.

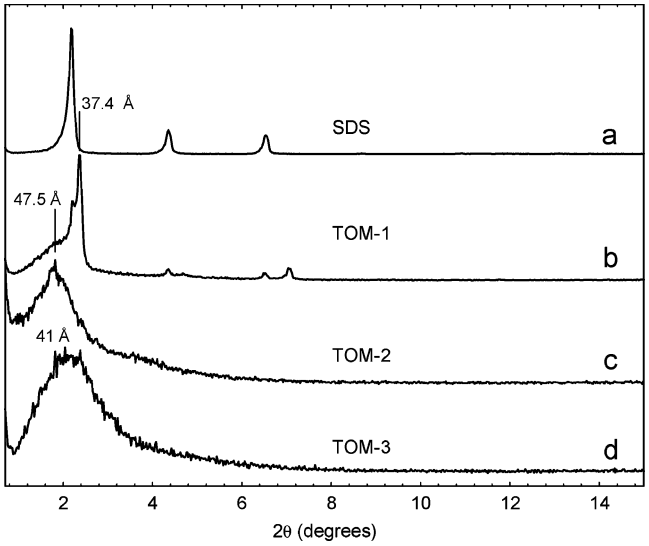

Figure 2. XRD patterns of (a) SDS, (b) TOM-1, (c) TOM-2, and (d) TOM-3 dried at 75 °C overnight.

substitution can be exploited in SANS to substantially change the contrast between the solvent and the solute components. By independently labeling the templated solute and solvent isotopically with hydrogen or deuterium, the scattering intensity as a function of solvent SLD can be measured. When the SLD of the fluid and solute components are matched ($\rho_m = \rho_s$), the scattering intensity will be nulled ($I(0)$). Hence, the SLD of the particles can be determined. The scattering length densities of $CH_3(CH_2)_{11}OSO_3Na$ and $CD_3(CD_2)_{11}OSO_3Na$ can be estimated from previously reported values.[34] In this study, we use well-established methods[35−37] and vary the SLD of the solvent by changing the C_2D_5OD/C_2H_5OH ratio in the solvent solution from 0 to 1. Also, by using both hydrogenated (*h*-TiDS) and deuterated (*d*-TiDS) precursors, the SLD of solute components could be varied. For a reaction time exceeding 12 h, a contrast variation series of SANS measurements for each template was made. The SANS patterns were measured by the small-angle diffractometer SAND at IPNS, Argonne National Laboratory. Form factors were fitted to the X-ray and neutron scattering data using the software supplied by Steven Kline of NIST.

Results and Discussion

TOM Characterization. *XRD.* Low-angle XRD patterns of products produced using metal (Ti)/dodecyl sulfate ratios (M/S) of 1−3 are shown in Figure 2. These products are termed TOM-*x*, where *x* represents the M/S ratio. The TOM-1 product (Figure 2b) contains two intense sharp reflections at $2\theta = 2.2$ ($d = 40.1$ Å) and 2.36° ($d = 37.4$ Å) and a series of higher angle reflections that are harmonics of these primary reflections. This powder pattern is similar to that of SDS shown in Figure 2a and suggests that, like SDS, the TDS-derived TOM-1 product comprises mostly lamellar phases. However, in addition to the sharp reflections due to SDS, a broad reflection is observed at $2\theta = 1.86°$ ($d = 47.5$ Å). Ordered lamellar phases are not observed in the powder pattern of TOM-2 (Figure 2c). Instead, only the low-angle broad component at $2\theta = 1.86°$ is observed in addition to a much weaker broad shoulder (Figure 2c) at around $2\theta \sim 3.3°$ ($d \sim 27$ Å). If the most intense reflection is the (100) reflection of a hexagonal cell then the unit cell *a* dimension should be given by $a = 2d/\sqrt{3} = 54.9$ Å. This would then mean that the (110) reflection of a hexagonal cell should occur at $d \sim 27$ Å which is close to the spacing estimated for the broad shoulder.

The XRD pattern obtained for TOM-3 (Figure 2d) contains a single weak low-angle peak indicating that the degree of order is lower than that for TOM-2. No other higher angle shoulder is observed here, and reflections due to crystalline titania are not observed either. These XRD results, therefore, support the formation of poorly ordered wormhole type surfactant−titania mesophases when Ti/DS is greater than or equal to 2. Such one-peak diffraction patterns are reminiscent of HMS[38] and MSU[39] mesoporous materials which have so-called wormhole frameworks and which are produced using neutral amine templates. The low-angle peak observed in the XRD patterns of the TOM materials cannot be considered as a Bragg peak of lattice planes reflecting the center-to-center distance of small highly uniform cubic or hexagonally packed anatase ($d_{101} = 3.516$ Å) or rutile ($d_{110} = 3.248$ Å) particles that diffract coherently because there is no evidence of such titania phases in the high-angle region of the XRD pattern.

Electron Microscopy. The three uncalcined mesoporous titania compounds were examined by TEM. What appear to be large primary particles are observed for all samples investigated. While no fringes could be observed for TOM-1, in certain particle orientations a striated fringe pattern with a spacing of about 28 Å could be discerned for the TOM-2 phase. Similar striated fringe patterns are observed more often than hexagonal fringe patterns in TEM images of hexagonal surfactant-templated ordered mesoporous silicate phases showing up to four XRD peaks. Similar striations have been attributed to the view at right angles to the hexagonal axis.[40]

(34) Berr, S. S.; Coleman, M. J.; Jones, R. R. M.; Johnson, J. S., Jr. *J. Phys. Chem.* **1986**, *90*, 6492.
(35) Iton, L. E.; Trouw, F.; Brun, T. O.; Epperson, J. E.; White, J. W.; Henderson, S. J. *Langmuir* **1992**, *8*, 1045.
(36) Dougherty, J.; Iton, L. E.; White, J. W. *Zeolites* **1995**, *15*, 640.
(37) Watson, J. N.; Iton, L. E.; Keir, R. I.; Thomas, J. C.; Dowling, T. L.; White, J. W. *J. Phys. Chem. B* **1997**, *101*, 10094.
(38) Tanev, P. T.; Pinnavaia, T. J. *Science* **1995**, *267*, 865.
(39) Bagshaw, S. A.; Prouzet, E.; Pinnavaia, T. J. *Science* **1995**, *269*, 1242.

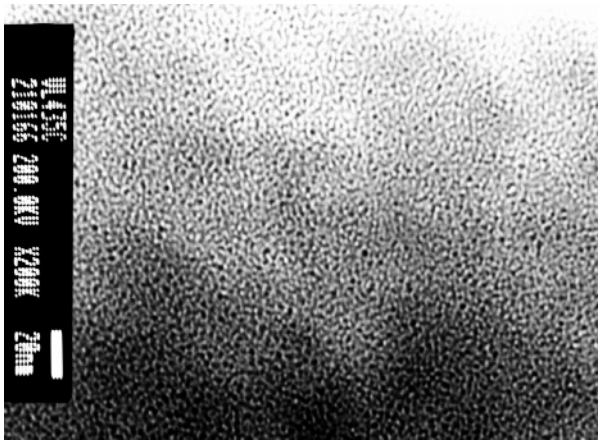

Figure 3. Bright field TEM image of vanadium exchanged TOM-3.

In other orientations a dappled fringe pattern is evident that is indicative of relatively uniform tubular pores that are poorly ordered. Similar fringes are often observed under certain diffraction conditions for MCM-41 phases possessing up to four XRD peaks or, more frequently, for poorly ordered MCM-41 (two XRD peaks). For uncalcined TOM-3 samples, only this kind of wormhole fringe pattern could be observed.

TEM analysis of MO_4^{2-}-exchanged TOM materials (M = V, Mo, W) dried at 70 °C indicated retention of the wormhole texture with an interpore spacing of about 30 Å (Figure 3). When such samples were calcined at 400 °C, a similar pore spacing was evident; however, the metal distribution varied from particle to particle. In general, regions of metal deficiency showed evidence of 50−100 Å anatase particles using dark field imaging. Selected area diffraction confirmed the anatase crystal structure of these particles. Sample regions with high metal concentrations showed disordered mesoporous texture and no evidence of anatase crystallites. These experiments show that anion exchange using molybdate, tungstate, or vanadate solutions remove all of the surfactant and generates mixed-metal oxide mesophases with modest thermal stability and pore dimensions that are somewhat smaller than the original Ti mesophase. We hypothesize that well-dispersed anionic metal species line the pores of the Ti mesophase, thereby stabilizing the framework and inhibiting to some extent the crystallization of anatase (see Supporting Information).

Infrared Spectroscopy. In this section we compare the Fourier transform infrared (FTIR) spectrum of TOM-3 with those of SDS and TDS and the spectrum of a Ti_8 cluster which forms from the reactant solution in low yield when only partial hydrolysis is permitted and the crystallization time is very long. This compound is only relevant in the present work inasmuch as it is a highly crystalline titanium oxo-alkoxysulfate compound whose structure is precisely known and can serve as a model for interpretation of FTIR and EXAFS data. The detailed synthesis and crystal structure of this Ti_8 cluster compound will be reported in a separate publication. Summary of the crystallography and the detailed FTIR band assignments of the Ti_8 cluster compound are included in the Supporting Information.

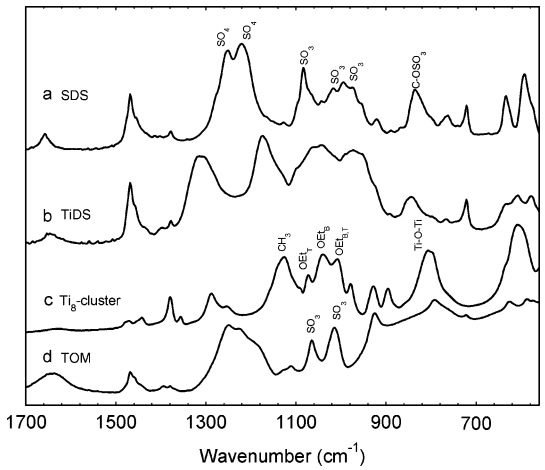

Figure 4. FTIR spectra of (a) SDS, (b) Ti-DS salt precursor, (c) Ti_8 cluster compound, and (d) TOM-4 material. Note that the intense bands at 1220 and 1250 cm^{-1} that are characteristic of $-OSO_3-$ in SDS are also present in the TOM phase.

FTIR spectra of the various related materials together with that of a TOM-3 are shown in Figure 4. The spectrum of dodecyl sulfate shown in Figure 4a has been previously assigned[41] and it is characterized by having two intense SO_4 stretching vibrations at 1253 and 1220 cm^{-1}. The spectrum of both the TDS precursor (Figure 4b) and the briefly described Ti_8 oxo-alkoxysulfate cluster compound (Figure 4c) are significantly different compared to that of SDS. In particular, the main SO_4 stretching vibrations appear to be significantly shifted to higher and lower frequencies indicating a significant change in the bonding about the headgroup. Unlike the FTIR spectrum of the precursor TDS compound, which presumably has a trivalent ion positioned close to the basal sulfate oxygen atoms, or the Ti_8 cluster, which contains no $C-OSO_3$ bond, the spectrum of the TOM product (Figure 4d) most closely resembles that of the SDS in terms of the SO_4 vibrations. In addition, some of the SO_3 vibrations around 1080 and 1025 cm^{-1} show some frequency shifts. The similarity of the FTIR spectrum of the TOM product with SDS may be considered definitive evidence that the sulfate headgroup remains bound to the hydrocarbon chain as in SDS rather than being indicative of an isolated SO_4 group as in the Ti_8 cluster compound we have described.

X-ray Absorption Spectroscopy. To further elucidate the nature of the bonding between the sulfate headgroup and the structural characteristics of the titanium oxide bonding in the wormhole framework, X-ray absorption spectra of uncalcined TOM-*x* materials with $x = 1$, 2, and 3 as well as nanocrystalline anatase (average particle size < 50 nm) were recorded at 298 K for comparison. Qualitative comparison of the Fourier transform (FT) data of the TOM-*x* materials with those of nanocrystalline anatase (Figure 5) indicates convincingly that the TOM materials have titanate frameworks in which the average local environment around the Ti atoms is not consistent with that of Ti atoms in anatase, rutile, brookite, or amorphous hydrous titanium oxides. Extraction of scattering atom identities and distances from the embedded Ti atom can be obtained using single scattering theory. Figure 5 shows the k^3-weighted EXAFS and the FT

(40) Chenite, A.; Le Page, Y.; Sayari, A. *Chem. Mater.* **1995**, *7*, 1015.

(41) Thompson, W. K. *Spectrochim. Acta, Part A* **1974**, *30*, 117.

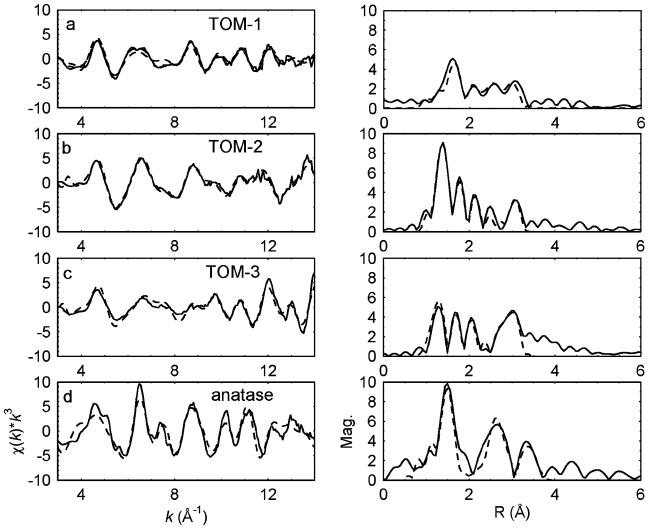

Figure 5. k^3-weighted Ti K-edge EXAFS (left) and FT (right) of (a) TOM-1, (b) TOM-2, and (c) TOM-3 samples dried at 70 °C and (d) nanocrystalline anatase. Experimental data are shown as the solid line, and the simulation using single scattering theory is shown as the dashed line. FT spectra have not been phase corrected.

Table 1. EXAFS Parameters for Nanocrystalline Titania (n-TiO_2) Compared with Uncalcined TOM-x Materials Determined Using Single Scattering Theory Using the Program XFIT[a]

sample	shell	N	R (Å)	σ^2 (Å^2)
n-TiO_2	O	3.4	1.94	0.005
	O	0.5	1.98	0.01
	Ti	1.9	3.03	0.006
	O	4.8	3.82	0.004
TOM-1	O	1.0	1.53	0.001
	O	1.0	2.05	0.001
	O	1.2	2.25	0.001
	S	1.3	3.28	0.006
TOM-2	O	1.6	1.62	0.001
	O	1.4	2.10	0.001
	O	1.2	2.30	0.001
	O	1.3	3.24	0.002
	S	1.0	3.1	0.004
TOM-3	O	1.0	1.67	0.005
	O	2.1	2.05	0.004
	O	1.4	2.25	0.004
	O	1.9	2.89	0.004
	S	1.3	3.29	0.002

[a] N = coordination number; R = distance; σ = Debye−Waller factor.

EXAFS of these data fitted using this approach. The fitting results are shown in Table 1 and indicate the presence of a very short Ti−O distance of about 1.6 Å for all the TOM-x materials that is not consistent with the Ti−O distances found in titania polymorphs which typically lie between 1.94 and 1.98 Å. Such short Ti−O distances are, however, observed in the previously described Ti_8 cluster compound. Still longer Ti−O bond distances are found in the TOM phases at about 2.3 and 3.2 Å that exceed both nearest and next-nearest neighbor distances in titania polymorphs. Indeed, the 3.2 Å distance is close to the distance found between titanium and the sulfur atoms of the coordinated sulfate in crystals of the Ti_8 oxo-alkoxysulfate cluster with distances around 3.21 Å (see Supporting Information). It is also to be noted that the intensity of the FT peak that has been ascribed to backscattering sulfur atoms is most intense in the TOM compound with the lowest M/S ratio and decreases in intensity as M/S increases. This is consistent with a diminishing contribution

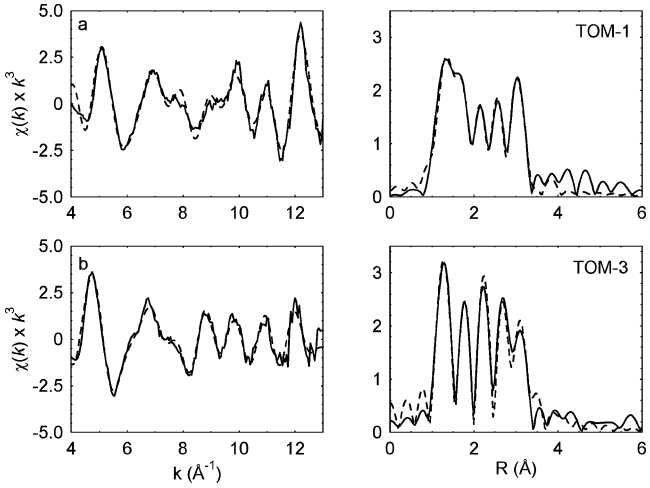

Figure 6. k^3-weighted Ti K-edge EXAFS (left) and FT (right) of uncalcined (a) TOM-1 and (b) TOM-3. Experimental data shown as solid line and simulation shown as dashed line. Fitting performed using IFEFFIT and multiple scattering theory with the Ti_4 atom of the Ti_8 cluster as the starting parameter.

Table 2. Ti−O Bond Distances in Angstroms for the Four Atoms in the Asymmetric Unit of the Ti_8 Cluster

Ti1	Ti2	Ti3	Ti4
1.758 18	1.777 18	1.782 91	1.624 22
1.835 93	2.008 28	1.792 15	1.757 04
1.986 2	2.041 99	2.005 04	1.906 86
2.035 59	2.042 25	2.030 16	1.940 69
2.047 37	2.935 24	2.068 49	1.959 71
2.100 85	2.129 87	2.210 39	2.052 17

of these atoms to the EXAFS. It is difficult to argue, therefore, on the basis of the present EXAFS data that the TOM materials in the uncalcined state have frameworks that resemble very strongly the bonding in titanium oxides. Instead, the bonding has a greater similarity to that which is observed in the cluster.

To further check the coordination environment of the Ti atoms in the TOM materials we have used multiple scattering theory (FEFFIT) and structural parameters derived from the structure of the Ti_8 cluster as a starting model to fit the EXAFS spectra of the TOM materials. Table 2 lists the Ti−O bond distances found for each of the four Ti atoms within the asymmetric unit of the cluster. It is apparent that in the cluster a wide variation of Ti−O bond lengths are observed ranging from bonds as short as 1.62 Å to as long as 2.21 Å. Knowing that the TOM materials contain such very short and long Ti−O bonds as deduced from the previous fitting we used the paths calculated using the FEFF 7 code for Ti atom number 4 in the Ti_8 cluster as the starting model (Table 2). The fitting model was kept as simple as possible, and only backscattering atoms with scattering amplitudes above a certain threshold were included. The results of the fitting to the TOM-1 and TOM-3 spectra are shown in Figure 6, and fitting values are provided in Table 3. The fits are excellent, and this lends some confidence to the model used. Support of these results could be obtained using ^{17}O solid-state NMR, but this could not be performed for this work.

Thermal Properties. The procedure employed here for the synthesis of TOM materials involves the preparation of a dried glassy gel on driving off solvent and initiating hydrolysis on exposure to a humidified air stream. The gel

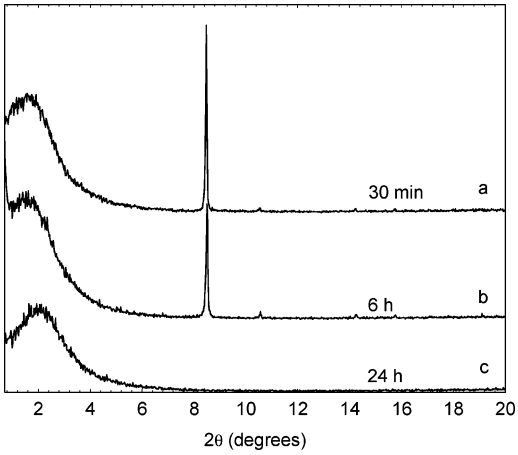

Figure 7. Effect of drying time at 75 °C on the low-angle diffraction pattern of TOM-3.

Table 3. Fitted EXAFS Parameters Using Multiple Scattering Theory Using the Program FEFFIT

sample	shell	*N*	*R* (Å)	σ^2 (Å^2)
TOM-1	O	2.2	1.57	0.0001
	O	2.1	1.72	0.0001
	O	3.7	2.10	0.010
	O	5.2	2.33	0.012
	O	4.7	2.87	0.0001
	Ti, S	7.4	3.40	0.002
TOM-3	O	3.1	1.57	0.001
	O	3.0	1.81	0.0004
	O	5.2	2.04	0.0002
	O	5.5	2.25	0.001
	O	4.9	2.92	0.000 01
	Ti, S	5.1	3.35	0.000 01

dried in this way is then further dried in a 75 °C oven for between 12 and 24 h. Because it became evident that some variability in the XRD pattern was being observed as a function of drying time, we chose to study drying in greater detail. The XRD patterns of TOM-3 products dried for increasing periods of time at 75 °C are shown in Figure 7. It is evident that after only brief drying (30 min), sharp reflections are observed in the XRD pattern, in addition to the broad low-angle reflections of the TOM phase. The intensities of these sharp reflections are reduced as the drying time increases, and they are eventually no longer observed. Such sharp reflections are obviously due to the presence of highly crystalline material in the sample present either as a separate phase or as an intimate part of the mesophase. The formation of the Ti_8 cluster compound that has been previously described is crystallized by partial hydrolysis of the precursor solutions used to make the TOM materials after extremely long periods of time. It is, therefore, possible that the crystalline phase observed in Figure 7 is related to cluster species of this type such as Ti_8. It should be noted that the XRD pattern observed here on drying possesses the main reflections of the powder pattern of the Ti_8 cluster compound (see Supporting Information). Recent publications[42] have also shown that nanoparticulate materials can be formed as the hydrolysis products of titanate precursor materials in the presence of surfactants. While it might be tempting to argue that the sharp XRD patterns being observed on partial drying are due to regions of the pore walls that have Ti_8-like building units, this is unlikely as the sharpness of the XRD peaks suggests highly crystalline material present together with the mesophase. This crystalline material does not survive the normal overnight drying protocol that was used for all sample preparations which results in decomposition of the cluster and possible structural rearrangements in the mesophase. This does not, however, preclude the existence of molecular building units within the pore walls that have structure similar to that of the Ti_8 cluster as indeed suggested by the EXAFS results.

Indeed, the ability to build up mesophase silicate materials using well-defined oligomeric silicate species was first demonstrated some time ago by Firouzi et al.[43] who exploited the double four ring silicate oligomer (cubic octomer) with formula $[H_nSi_8O_{20}]^{(8-n)-}$, where *n* represents the number of chemical bonds formed by a given Si atom to *n* other adjacent Si atoms. Subsequently, molecular clusters such as $Ti_{12}O_{16}(OPr^i)_{16}$, $Ti_{16}O_{16}(OEt)_{32}$, and $Ti_{18}O_{22}(OBu^n)_{26}(acac)_2$ have been used as precursors to assemble textured titanate-organic hybrid materials[44] by interaction with the various complexing groups in BCs and dendrimers. In the present case the identification of framework bonding in TOM materials, that is, Ti_8-like, relies mostly on EXAFS evidence, and further substantiation could have been obtained through the use of ^{17}O NMR but was not possible for this work. Clearly, if such Ti_8-like bonding does exist in the condensed TOM framework, then it may have originated from the hydrolysis of the OPr and OEt bonds in Ti_8, and the following formation of hydroxyl bridges is required; this would distort somewhat the structure of the original Ti_8 unit.

Nitrogen adsorption−desorption isotherms of washed or unwashed TOM-3 materials prior to calcination were typically of type I (Figure 11a) and gave surface areas close to zero indicating that any pores in these materials are not accessible to nitrogen because they are filled with surfactant. It was not possible to calcine TOM-1 or TOM-2 to temperatures above 100 °C without causing total decomposition and eventually formation of nanocrystalline anatase. In fact, TOM-1 melts at temperatures below 80 °C. However, when TOM phases with $2.5 < x < 3.5$ are calcined in air at temperatures below 400 °C low-angle reflections are preserved in the XRD pattern. Thermal analysis data are reported in the Supporting Information and show complete removal of surfactant by this temperature.

XRD patterns of as-prepared TOM-3 materials heated in air at increasing temperatures are seen in Figure 8. For the sample heated at 300 °C (Figure 8b), a pronounced low-angle reflection is observed with a *d* spacing that is somewhat larger than that of the sample dried at 70 °C. However, there is no reflection from crystalline titania phases in this pattern which is consistent with the existence of only a wormhole mesophase. Lattice expansion may be due to rearrangement of the pore wall material on heating. Calcination at 400 °C

(42) Dag, O.; Soten, I.; Celik, O.; Polarz, S.; Coombs, N.; Ozin, G. A. *Adv. Funct. Mater.* **2003**, *13*, 30.

(43) Firouzi, A.; Kumar, D.; Bull, L. M.; Besier, T.; Sieger, P.; Huo, Q.; Walker, S. A.; Zasadzinski, J. A.; Glinka, C.; Nicol, J.; Margolese, D.; Stucky, G. D.; Chmelka, B. F. *Science* **1995**, *267*, 1138.

(44) Soler-Illia, G. J. de A. A.; Rozes, L.; Boggiano, M. K.; Sanchez, C.; Turrin, C.-O.; Caminade A.-M.; Majoral, J.-P. *Angew. Chem., Int. Ed.* **2000**, *39*, 4249.

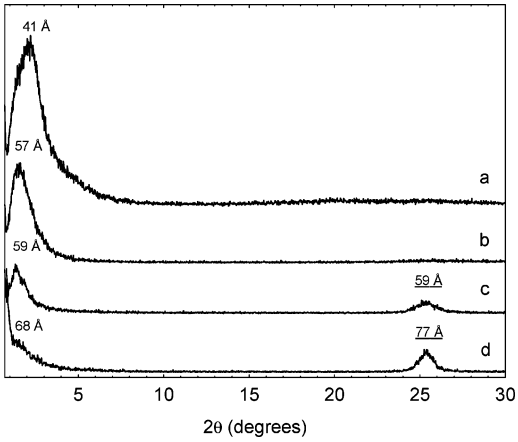

Figure 8. Effect of various thermal treatments on the XRD pattern of TOM-3 materials (a) dried at 75 °C and heated in air at (b) 300, (c) 400, and (d) 500 °C. The high-angle reflection at about 25.4° 2θ is due to anatase crystallites, and the underlined angstrom value above the peak is the particle size calculated using the Scherrer equation.

(Figure 8c) yielded a weaker low-angle reflection in addition to a high-angle reflection at 25.4° 2θ (d = 3.52 Å) corresponding to the most intense (101) reflection of nanocrystalline anatase. Thus, just after the removal of the organic materials the system evolves to a collection of anatase nanoparticles. For the sample heated at 500 °C there is further reduction in the intensity of the low-angle reflection and intensification and narrowing of the anatase (101) reflection. The average crystallite size calculated using the Scherrer equation was 77 Å, and TEM observations (not shown) confirmed the existence of anatase crystallites of about this size. The nitrogen adsorption isotherm of the TOM-3 phase calcined at 500 °C is of type IV showing only a slight hysteresis and having a shallow inflection at low P/P_0 indicative of small pores. BJH analysis gave an average pore size of 27 Å for this sample while the BET surface area was 128 m^2/g. The particle diameter calculated from this surface area under the assumption of spherical particles was 116 Å which is much larger than the value of 77 Å calculated from the broadening of the 101 reflection. In contrast, for anatase nanoparticles of different sizes synthesized through peptization of a titanium hydrolyzate formed from titanium isopropoxide by the method of Shklover et al.[45] it was possible to independently calculate particle diameters from the surface area, the anatase 101 peak broadening, and the low-angle XRD peak, which agreed to within 10%. The isotherm shape and the smaller than expected surface area for 61 Å particles obtained for calcined TOM-3 indicates that the assumption of a uniform spherical particle morphology is incorrect for the 500 °C heated sample. While the stability of the as-prepared TOM-3 material is clearly limited, some wormhole mesoporosity may be retained even at temperatures as high as 500 °C.

Ion Exchange and Surfactant Removal. While calcination of as-synthesized materials at temperatures exceeding 400 °C yielded modest mesoporosity, this porosity is probably mostly due to the packing of anatase nanocrystals presumably

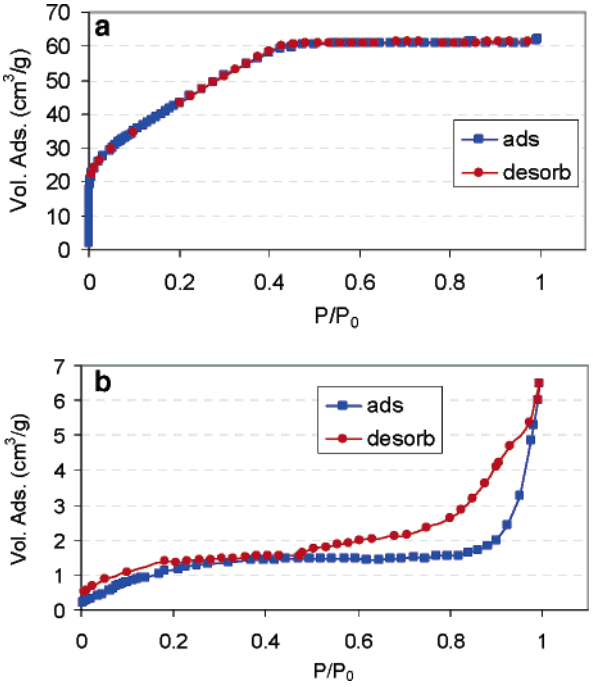

Figure 9. Nitrogen adsorption (■) and desorption (●) isotherms of TOM-3 exchanged with (a) 40 and (b) 200 mmol/L molybdate solutions and heated to 400 °C.

containing sulfate. Therefore, more mild methods of template removal were required to extract the sulfate surfactant from these materials. Because the surfactant is anionic, one of these involved contacting the as-synthesized titania mesophase with solutions of oxyanions of vanadium, molybdenum, and tungsten to afford heterostructured mesoporous oxides. Figure 10a shows the XRD pattern of a TOM-3 sample exchanged using a 40 mM sodium molybdate solution (pH = 6.5) followed by washing with Milli-Q water and drying at 70 °C. The XRD pattern was similar to that of the untreated material (Figure 9a) showing only a single broad low-angle reflection with a spacing between 40 and 45 Å. Release of surfactant from the Ti mesophase during the washing process was evidenced by extensive foaming and then the formation of two liquid phases. EDX analysis of samples treated in this way and dried at 65 °C showed Mo concentrations that were proportional to the concentration of the molybdate solution used for the ion exchange and concomitant loss of sulfur. Microanalysis (C, H, S) confirmed almost complete removal of sulfur. Calcination of the Mo-exchanged sample at temperatures exceeding 300 °C yielded a shift in the low-angle reflection to lower angles and the crystallization of some anatase. For the case of the sample shown in Figure 10b, however, the average crystallite size determined from the anatase (101) reflection was about 36 Å which is about half that of the low-angle reflection (65 Å), suggesting that such samples retained a degree of wormhole texture. Indeed, type IV adsorption isotherms can be obtained after calcination at temperatures between 300 and 400 °C with little or no hysteresis (Figure 9a). BJH analysis indicates average pore diameters of about 30 Å while surface areas were around 170 m^2/g.

When Ti mesophase samples are exchanged with concentrated molybdate solutions (e.g., 0.20 M) and the sample is heated to 400 °C in air, a profound transformation occurs in

(45) Shklover, V.; Nazeeruddin, M. K.; Zakeeruddin, S. M.; Barbe, C.; Kay, A.; Haibach, T.; Steurer, W.; Hermann, R.; Nissen, H. U.; Gratzel, M. *Chem. Mater.* **1997**, *9*, 430.

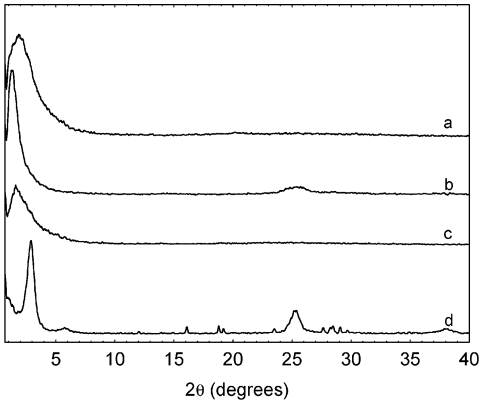

Figure 10. XRD patterns of (a) TOM-3 exchanged using a 40 mM sodium molybdate solution, (b) sample from part a calcined at 400 °C in air, (c) TOM-3 exchanged using a 200 mM sodium molybdate solution, and (d) sample from part c calcined at 400 °C.

the XRD pattern (Figure 10d). A relatively sharp and intense reflection is observed at 30.3 Å, and a weak peak with similar fwhm is observed at 15.3 Å. Also present in the pattern are peaks from nanocrystalline anatase with a particle diameter of 90 Å. Although our instrumentation limited us to the low-angle region above 0.7° 2θ there is some evidence of a peak at about 87 Å. This pattern also contains sharp reflections from a Mo oxide phase. In fact, the pattern of sharp reflections matches reasonably well that of $Na_2Mo_2O_7$. The N_2 adsorption isotherm of this sample (Figure 9b) is clearly of type I which is characteristic of nonporous materials, and the surface area is <4 m^2/g.

At this point our data are clearly consistent with the formation of mesoporous titanate material with a predominantly disordered wormhole pore arrangement. The following section will deal with the mechanistic aspects leading to the formation of this pore system.

Formation Process. The literature on surfactant templating points out the fact that the mechanisms which control the formation of these self-assembling systems are many, varied, and system dependent.[46,47] It is in many respects quite understandable that there is unlikely to exist a unique mechanism for the bewildering array of possible chemistries used to generate mesophases. The types of interactions between surfactant molecules and molecular precursors depend on the precise nature of the solution precursor species and the way these species interact with the hydrophilic and hydrophobic functional groups of a particular type of surfactant. In the case of molecular transition metal centers containing water, hydroxyl groups, alkoxides, and the like in their coordination sphere, the nature of the precursor complex can be extremely varied and suitable changes in structure could lead to significant differences in interaction parameters. Moreover, if this interaction is strong, such as in the case where the surfactant headgroup complexes the metal center, then the entire complex (surfactant−molecular metal complex) can be considered the headgroup, and the behavior of the system need not resemble in any way that of the parent surfactant.

SAXS and SANS techniques are ideal techniques for elucidating surfactant self-assembly and sol−gel processes, and they are routinely applied. They have also been applied in studying hydrolysis of titanium alkoxides in the absence of surfactants[19,48] because the dimensions of titanium clusters and nanoparticles can fall within the length scale probed by small-angle scattering techniques. More recently, such techniques have been applied to study mechanisms of metal oxide self-assembly in the presence of a range of simple and BC surfactants. For instance, the assembly of aluminum oxide mesophases using the anionic surfactant SDS,[49] silicate mesophases using simple and BC surfactants, and zirconium sulfates have been studied.[50] In the case of mesoporous titanium and silicon oxide thin films prepared from acidic ethanolic solutions of $TiCl_4$ and BC templates ($TiCl_4$/BC/EtOH/H_2O system) with low water contents deposited using dip coating (EISA), chemical reactions also occur on relatively short time scales of the order of seconds or minutes. To follow the rapid chemical changes occurring in such chemical systems one must use techniques that probe the system on short time scales relative to the reaction coordinate. Thus, time-resolved SAXS at grazing incidence angles have been applied with a data acquisition rate of typically a few seconds to observe the film formation process.[15,51,52] In such experiments the first Bragg scattering or correlation peak is observed within the first few tens of seconds for silicates and hundreds of seconds for titanates after film formation. Such a correlation peak is indicative of the commencement of aggregation of, or correlation between, micelles possibly toward a wormhole mesophase structure. A wormhole mesophase structure may imply aggregation of spherical, cylindrical, prolate, or other shaped micellar objects that have no order with respect to one another. What is subsequently observed in these dip coated thin film systems on drying is a progressive ordering with expulsion of volatile components and ingress of water. The region of time space prior to the appearance of the correlation peak and the formation of aggregates in the titanate system is seldom considered because no Bragg scattering and, therefore, no order is observed. It is, however, certainly not the case that the system does not evolve during this initial time interval. Rather, the self-assembly process, as well as hydrolysis and condensation reactions, may well and truly begin. While the nature of the initial micellar objects has never been defined in the case of titanate film or bulk material formation, particularly for the $TiCl_4$/BC/EtOH/H_2O system, an excellent SAXS study of the evolution of the bulk TEOS/P123/HCl/H_2O system during the preparation of SBA-15 has been carried out by Flodström et al.[47] In this study the nucleation of spherical P123−silicate

(46) Patarin, J.; Lebeau, B.; Zana, R. *Curr. Opin. Colloid Interface Sci.* **2002**, *7*, 107.
(47) Flodström, K.; Wennerström, H.; Teixeira, C. V.; Amenitsch, H.; Lindén, M.; Alfredsson, V. *Langmuir* **2004**, *20*, 10311.
(48) Blanchard, J.; Ribot, F.; Sanchez, C.; Bellot, P.-V.; Trokiner, A. *J. Non-Cryst. Solids* **2000**, *265*, 83.
(49) Forland, G. M.; Samseth, J.; Gjerde, M. I.; Hoiland, H.; Jensen, A. O.; Mortensen, K. *J. Colloid Interface Sci.* **1998**, *203*, 328.
(50) Ne, F.; Testard, F.; Zemb, Th.; Grillo, I. *Langmuir* **2003**, *19*, 8503.
(51) Cagnol, F.; Grosso, D.; Soler-Illia, G. J. de A. A.; Crepaldi, E. L.; Babonneau, F.; Amenitsch, H.; Sanchez, C. *J. Mater. Chem.* **2003**, *13* (1), 61.
(52) Grosso, D.; Babonneau, F.; Sanchez, C.; Soler-Illia, G. J. de A. A.; Crepaldi, E. L.; Albouy, P. A.; Amenitsch, H.; Balkenende, A. R.; Brunet-bruneau, A. *J. Sol.-Gel Sci. Technol.* **2003**, *26*, 561.

hybrid micelles and their evolution to a two-dimensional hexagonal mesophase were evidenced.

The chemistry used in the present work to prepare TOM materials has been deliberately designed to severely hinder both hydrolysis and condensation. Even the first oxidation step, where the solution undergoes a color change uniformly from burgundy to yellow, requires several hours. Therefore, it is expected that in this initial stage, very little hydrolysis or condensation occurs. Such slow chemical changes facilitate the study of the system using even laboratory-based small-angle scattering techniques, and here we have been able to apply these in situ. In addition, these scattering techniques probe length scales that are ideal for following the initial stages of condensation and can furnish information on the size and shape of molecular and nanoscale metal oxide objects in the solutions.

It is clear that in the anhydrous state the present solutions consist of at most very small titanium alkoxide clusters or oligomers having mostly alkoxy groups in their periphery and discrete surfactant molecules. The introduction of water results in hydrolysis of these small oxo-alkoxy titanium clusters which become increasingly hydrophilic, and this must modify the interaction with the headgroup of the sulfate surfactant. Expulsion of alcohol induced by hydrolysis then permits the entry of sulfate from the surfactant into the coordination sphere of the titanium centers.

The SAXS of a freshly prepared Ti-DS/EtOH/$Ti(OPr)_4$ solution as a function of reaction time is shown in Figure 11a. At the start of the reaction, no scattering is observed from the system, which is consistent with the presence of discrete surfactant molecules and perhaps oxo-alkoxy titanium clusters or oligomers that are either too small or too large to give rise to any significant scattering in the q range probed. The first perceptible scattering is observed from the system after about 2 h of reaction (Figure 11a). The intensity measured at the same q value is plotted as a function of reaction time in the inset to Figure 11a and shows a power law dependence of the kinetics. Unlike the studies of the self-assembling Zr−CTAB system by Ne et al.,[50] no obvious incubation time can be observed on the time scale of the reaction being interrogated here. However, the time resolution of the present experiments is low compared to that employed by Ne et al. while reaction rates are far more protracted in duration, lasting some 48 h. In the present experiments a significant increase in scattering is observed after 5 h.

In Figure 11b are shown SAXS data taken at selected time intervals after the start of reaction. The data have been fitted with the general Guinier expression as follows:

$$I(q) = (I_0/q^n)e^{-q^2d^2}$$

Here, d gives the characteristic dimension of the scattering entity and n depends on the scattering geometry with $n = 0$, 1, and 2 corresponding to globular, needle, and plate geometries. It can be seen that up to 11 h from the start of reaction the data can be fitted well with $n = 0$. After about 15 h of reaction the data can no longer be fit well with $n = 0$ (spheres), while at longer times, excellent fits could be

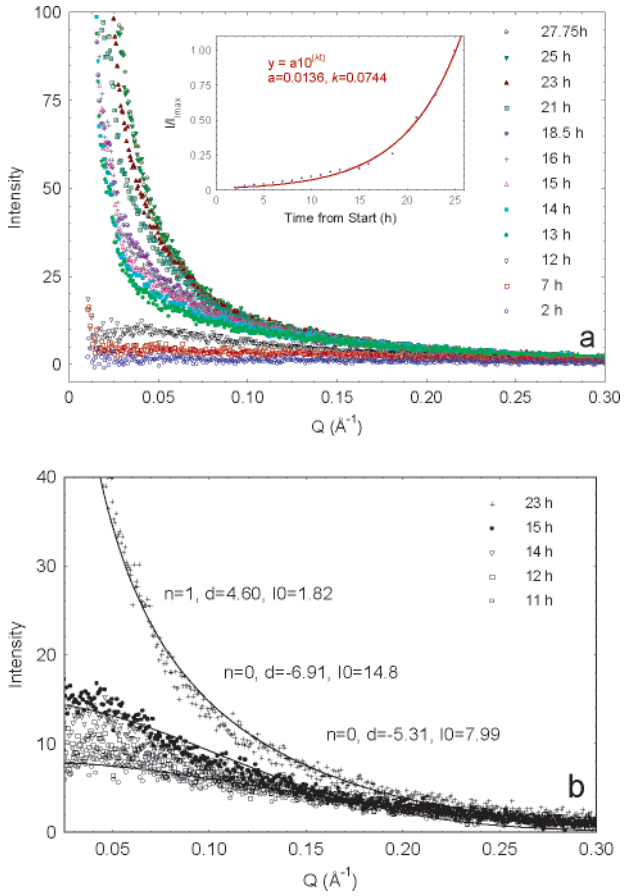

Figure 11. (a) Scattering intensity as a function of Q for selected times from the start of reaction. The inset shows the variation of intensity with reaction time. (b) Guinier fits for selected data sets from part a. Only the 11, 15, and 23 h data have been fitted (solid lines).

obtained with $n = 1$ (cylinders). This model independent approach, therefore, convincingly demonstrates the transformation from spherical to rod shaped scattering entities. It is important to note that SAXS experiments carried out using $Ti(OPr)_4$/EtOH solutions containing no surfactant failed to show any significant scattering after times for which surfactant-containing solutions showed significant scattering. From this we can infer that the scattering entities contain surfactant rather than being simply metal oxide nanoparticles.

In Figure 12 are shown selected SAXS data fitted to various form factors. While the data after short reaction times up to 11 h are reasonably well fitted with a sperical form factor, when the reaction time exceeds about 11 h, a spherical form factor no longer adequately represents the data and a cylindrical form factor needs to be employed. This supports the model independent Guinier fits in Figure 11. Form factor fits allow the extraction of the radius and length of the scattering objects. At reaction times in the range of 2−11 h the spherical radius progressively increases from 8 to just under 14 Å just prior to a transformation to cylindrical micelles (Figure 13). Thus, the spherical micelles appear to grow as a function of reaction time. Beyond 11 h, a spherical form factor no longer models the data as well and a transformation to cylindrical objects occurs. These cylindrical micelles also grow, increasing in both radius and length.

There are several ways in which growth of micellar objects can be envisaged to occur. Two possible extremes are either

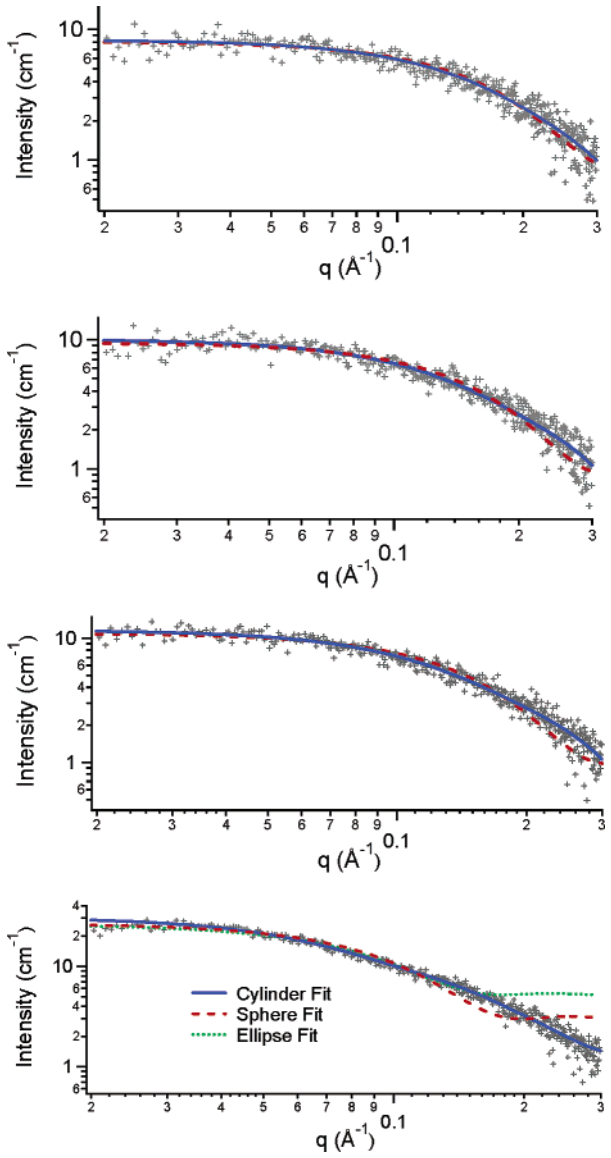

Figure 12. SAXS after 11, 12, 13, and 18.42 h of reaction showing that the sphere form factor better represents the data. Solid blue = cylinder, dashed red = sphere, and dotted green = ellipse.

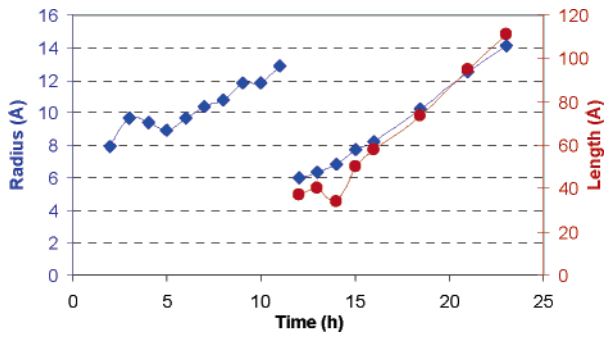

Figure 13. Results of fitting of the SAXS data as a function of time. At about the 11 h mark a spherical form factor is no longer applicable, and a cylinder fit is used so that two dimensions are required.

addition or accretion of oxo-alkoxy titanium species to the micellar palisade region and/or through a straightening of the hydrocarbon chain of the surfactant molecules, which in any case are initially significantly contracted compared to the value of 16.7 Å expected for a fully extended hydrocarbon chain.[34] The precise nature of the transition, whether

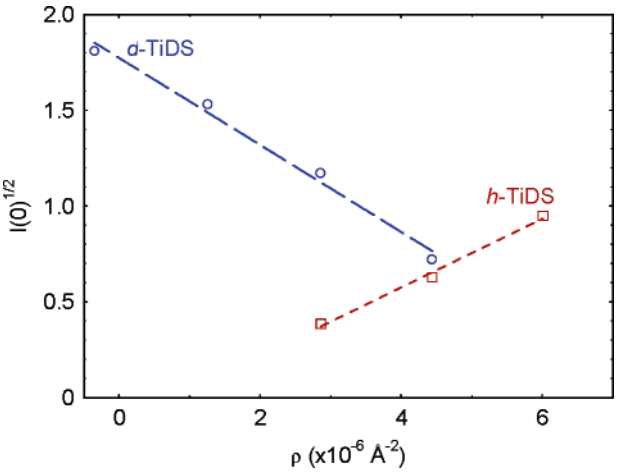

Figure 14. Contrast variation plots of SANS intensities for Ti-DS/EtOH/TIP solutions reacted in excess of 12 h at 30 °C for the *h*-TiDS (□) and *d*-TiDS (○) templates. Lines represent linear fits to the data.

abrupt or progressive, is too difficult to gauge with the 1 h time slices available using our instrumentation. However, from about 11 h it appears that cylindrical objects grow both in radius and in length finally reaching radii of about 14 Å and lengths of about 100 Å just prior to gelation. Of all the metal oxide systems assembled from surfactants, in only a few instances have sphere-to-rod transitions been observed. Some recently described and particularly relevant systems include the Na-silicate/CTAC/TMA/H_2O system by Lee et al.,[53] the $Al(NO_3)_3$/SDS/urea/H_2O system investigated by Sicard et al.,[54] and most recently, the $ZrOCl_2$/CTAB/H_2O system studied by Ne et al.[50]

While the SAXS data indicate first the appearance of a spherical micellar structure followed by transformation to cylindrical objects, these objects can be anything from pure SDS micelles to pure titanate structures. Information on the identification of these scattering objects can be provided by SANS contrast variation experiments which were carried out following reaction to the point at which cylindrical objects were established.

The contrast match data (plot of $\sqrt{I(0)}$ versus solvent SLD) is shown in Figure 14 for both the deuterated (*d*-TiDS) and hydrogentated (*h*-TiDS) dodecyl sulfate Ti(III) precursor-containing solutions. In such experiments the SLD of the solvent is progressively altered by varying the proportion of undeuterated and deuterated ethanol (d_6-EtOH) solvent. It can be seen that the intensities extracted by extrapolation of the Guinier plots to zero *q* decrease and increase in intensity for the *d*-TiDS and *h*-TiDS solutions, respectively, as a function of the SLD of the solvent. This linearity and trend reversal as a function of the isotopic state of the solution demonstrates definitely that the scattering objects being detected here contain surfactant. From linear fits to these data the contrast match points are determined to be 0.45×10^{-6} and 7.45×10^{-6} Å^{-2} for *h*-TiDS and *d*-TiDS, respectively. Such values are of the order of those estimated for $CH_3(CH_2)_{11}OSO_3$ and $CD_3(CD_2)_{11}OSO_3$, respectively,

(53) Lee, Y. S.; Surjadi, D.; Rathman, J. F. *Langmuir* **1996**, *12*, 6202.
(54) Sicard, L.; Lebeau, B.; Patarin, J.; Zana, R. *Langmuir* **2002**, *18* (1), 74.

which implies that the scattering objects are predominantly dodecyl sulfate micelles with limited, if any, contribution from Na or Ti.

In the present experiments when the C_2D_5OD/C_2H_5OH ratio is altered to change the contrast of the solvent, the introduced ethanol molecules in the deuterated or hydrogenated form actually participate in the reaction with Ti−alkoxy complexes via alcohol exchange. It is also to be noted that water introduced into the system when humidified air is admitted for a period of at least 12 h to effect the sphere-to-rod micellar transition observed by SAXS also participates in the reaction with the metal center through hydrolysis. Thus, the effective solvent is composed of three components, $Ti(OPr)_4$, ethanol, and water, which react. Both the alcohol introduced as a mixture of C_2D_5OD/C_2H_5OH and water are able to interact with the Ti metal center and displace PrOH from the Ti coordination sphere, and this is volatilized. A concomitant degree of condensation of the metal complex to form small oligomers probably also occurs, but the "tenuous objects" identified by Blanchard et al.[48] are not evidenced on the basis of the difference in the scattering curves. Also, as previously mentioned, solutions with the same composition as those used to produce TOM materials but which do not contain surfactant do not give rise to any significant scattering. This clearly suggests that such objects are not favored under our synthesis conditions or lie outside our q window. Therefore, in the particular system addressed here, the solvent can be considered as the reaction product of $Ti(OPr)_4$, ethanol, and water to give probably small oligomers. The contrast match point must, therefore, represent the SLD of the surfactant against a background of oxo-alkoxy titanate clusters and ethanol. This situation seems more consistent with the growth by chain elongation mechanism depicted in Figure 15b as opposed to growth by the accretion model (Figure 15a). This would also seem to be supported by the fact that gelation, as opposed to precipitation, is what is observed experimentally. Growth by accretion has been demonstrated to occur using dynamic light scattering and SAXS during the synthesis of MSU-X, a wormhole mesoporous silicate prepared via a two-step process using the surfactant Turgitol ($CH_3(CH_2)_{14}(EO)_{12}$).[55]

Dodecyl sulfate is one of the simplest and most studied ionic surfactants. It has been generally accepted that the binary system, SDS/water, presents the phase sequence I (isotropic)−direct H (hexagonal)−LR (lamellar) with increasing concentration, with several intermediate phases between H and LR, all showing long-range positional order.[56,57] Thus, even the binary system is relatively complex which is why it has been extensively studied over a long period of time. However, recently even the existence of the basic phases has been called into question.[58] Addition of salts such as NaCl or KBr cosolvents and cosurfactants can profoundly change the size and shape of the micelles, and this has also been extensively studied.[49,59] In the present system the complexity is further increased because of the complex nature of the "solvent" system, which evolves over time. It is, therefore, indeed both surprising and gratifying that our results nevertheless lend themselves to relatively straightforward interpretation.

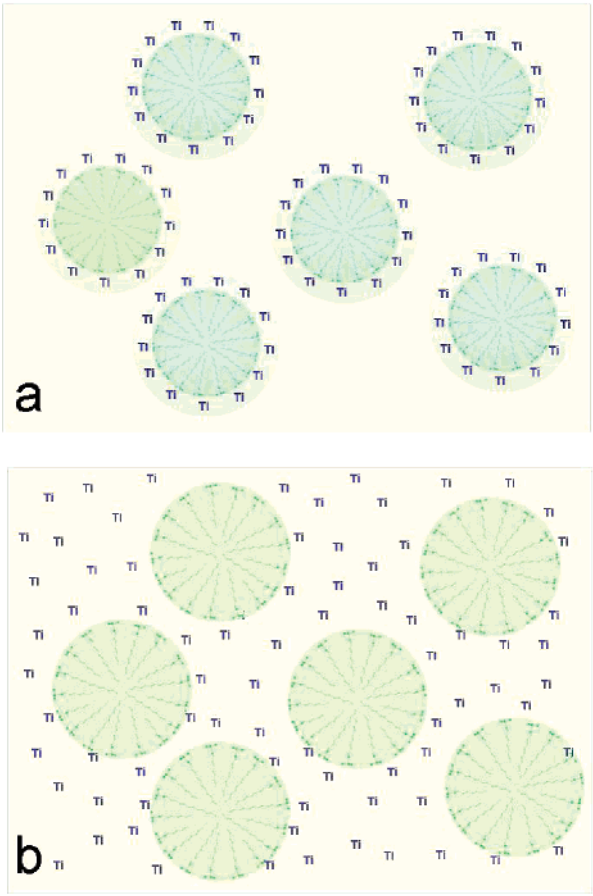

Figure 15. Two possible models for the formation of TOM material: (a) growth by accretion of oxo-alkoxy titanate species within the palisade region and (b) growth by straightening of the dodecyl sulfate chain within a structureless solution background.

Therefore, the reaction mechanism which can be proposed for the TOM self-assembly is that at $T = 0$ there are only individual surfactant molecules in solution which have not aggregated. It is important to also note that at this point the absence of large Ti-containing oxo-alkoxy clusters were not observed. The initial absence of micelles is in accordance with expectations for the behavior of this surfactant in ethanol. The introduction of water from the vapor phase initiates hydrolysis so that the Ti complex becomes less and less hydrophilic and interacts more strongly with the micelle headgroup layer while OPr and OEt are removed from solution as the respective alcohols. At a certain critical point in the reaction coordinate, the enhanced interaction of the headgroup and Ti−oxo complexes provokes a sphere-to-rod transition.

Conclusion

The first part of this paper has focused on reporting a novel synthetic procedure for the preparation of a new mesostruc-

(55) Boissiere, C.; Larbot, A.; Bourgaux, C.; Prouzet, E.; Bunton, C. A. *Chem. Mater.* **2001**, *13*, 3580.
(56) Kekicheff, P. *J. Colloid Interface Sci.* **1989**, *131*, 133.
(57) Kekicheff, P.; Grabielle-Madelmont, C.; Ollivon, M. *J. Colloid Interface Sci.* **1989**, *131*, 112.
(58) Bergstrom, M.; Pedersen, J. S. *J. Phys. Chem. B* **1999**, *103*, 8502.
(59) Kumar, S.; David, S. L.; Aswal, V. K.; Goyal, P. S.; Kabir-ud-Din *Langmuir* **1997**, *13*, 6461.

tured titanium oxide material and its detailed characterization. No attempt has been made to describe the chemistry of the Ti^{3+} dodecyl sulfate salt precursor which itself is likely to have interesting surfactant properties.

The TOM materials consist of poorly ordered surfactant-filled channels permeating a continuous titanium−oxygen bonding network. The channel structure is that of a typical wormhole mesophase rather than a well-ordered hexagonal or cubic phase as is the case for MCM-41 or MCM-48. Indeed, similar silicate materials displaying a single low-angle XRD peak were initially reported some time ago, and titanate analogues have subsequently also been reported. While one advantage of using dodecyl sulfate is the low cost, another is the easy extraction of the surfactant by anion exchange. The ion exchange process offers potential for pore size control because introduction of the second oxide proceeds uniformly and in a progressive manner. Indeed, this facile ion exchange shows that the pore system in the TOM materials is quite accessible.

The XRD and EXAFS evidence presented here suggests that in the dried state the pore walls have an unusual structure that more closely resembles the bonding in the Ti_8 cluster compound than in bulk titania (anatase or rutile). It is hypothesized that this structure is somewhat preserved on dehydration of the materials at mild temperatures. Thus, the sulfate is presumed to be bound to the titanate framework via three basal oxygen atoms of the sulfate group as it is observed in the Ti_8 cluster compound. When the sulfate is removed we speculate than an imprint is left on the titanate surface that disposes it to sorb similarly configured oxo-anions.

The formation of a mesostructured Ti−oxide with wormhole porosity[60] that possesses anion exchange properties has significant implications across a broad range of application areas. First, ion exchange of itself implies potential uses in the recovery of metals that exist as simple or complex anions in various solution conditions, for example, MoO_4^{2-}, WO_4^{2-}, VO_4^{2-}, CrO_4^{2-}, and TeO_4^{2-}, to name only a few. Anion exchange of hydrous titanium oxide is not usually expected to occur to any significant extent at pH values greater than about 7 (the isoelectric point is 4.7 for hydrous titania and 6.2 for anhydrous titania). Indeed, comparative ion exchange experiments have shown that TOM sorbs an order of magnitude more molybdate and tungstate than hydrous amorphous titania under the same conditions. Conversely, TOM sorbs <100 μg/g of Cu^{2+} from a 0.1 M $CuNO_3$ solution, while under comparable conditions, hydrous amorphous titania and nanocrystalline rutile sorb 3300 and 6300 μg Cu/g, respectively. These vastly differing ion exchange properties confirm that the surface structures (and, hence, surface acidities) of TOM and conventional materials are quite different. A detailed study of the adsorption of arsenate and other anions by these materials will be reported in a forthcoming publication.

Like other surfactant templated mesophase materials report so far, bulk TOM powders have limited thermal stability. Materials exchanged with oxo-anions of Mo, V, and W when calcined at temperatures of up to 400 °C are not monophasic but rather consist of discrete regions with poorly ordered mesoporosity and regions comprising mainly packed titania nanocrystals. These nanocrystalline regions will possess their own mesoporosity that is not expected to be unlike that of the noncrystalline mesoporous regions.

The ability to achieve, in a facile way, a high level of dispersion of the catalytically active metal oxide on the internal pore surfaces of a mesoporous titania implies that useful catalytic properties could be envisaged, for instance, in the selective reduction of nitric oxides where the commercial catalyst is titania-supported vanadia. In the area of photovoltaics, the ability to bind anionic metal clusters opens up vistas of opportunity in surface sensitization and possibly the ability to tune the photoresponse of titania to make more efficient use of the solar spectrum.

The second part of this paper has focused on achieving a detailed understanding of the formation process of the TOM materials. In some respects the synthetic conditions are not unlike those used in the preparation of titania thin films using water containing ethanolic solutions of $TiCl_4$ and BCs. In the present case, by severely slowing down the reaction rates through the use of Ti(III) in the precursor solution, we are able to probe the solution state in a detailed manner using laboratory-based SAXS and SANS and evidence the onset of micellization. These experiments show definitively first the formation of spherical micelles and then the occurrence of the sphere-to-rod transition as the reaction proceeds and the hydrophilicity of the metal center promotes greater interaction with the surfactant headgroup.

Acknowledgment. V.L. is particularly indebted to his coauthor and friend J.N.W., for his input of scattering expertise more than 4 years after the scattering experiments were first performed. Useful discussions with Dr. W. Bertram of ANSTO on various aspects of the scattering data and assistance with TEM from Dr. David Mitchell of ANSTO are also acknowledged. V.L. is particularly grateful to Dr. Galo Soler-Illia for good-humored discussions and valuable insights. X-ray absorption experiments were supported by the Australian Research Council. Access to the Photon Factory was provided by the Australian Synchrotron Research Program, which has been funded by the Commonwealth of Australia via the Major National Research Facilities Program, which also provided funding for experiments to be undertaken at IPNS, Argonne National Laboratory, Argonne, IL. This work benefited from the use of the Intense Pulsed Neutron Source which is funded by the U.S. Department of Energy, Office of Basic Energy Science, and other Department of Energy Programs under Contract No. W-31- 109-ENG-38 to the University of Chicago. We thank Dr. Steve Kline from NIST for his SANS analysis software and Denis Wozniak for his assistance at IPNS. Finally, we thank Professor John White of the Australian National University for making his X-ray scattering instrumentation available.

Supporting Information Available: Structure information including diagrams and tables of crystal data, structure solution and refinement, atomic coordinates, and bond lengths and angles for the Ti_8 cluster compound. FTIR spectral assignments of Ti are also provided (PDF). This material is available free of charge via the Internet at http://pubs.acs.org.

CM051255K

(60) Breulmann, M.; Coelfen, H.; Hentze, H. P.; Antonietti, M.; Walsh, D.; Mann, S. *Adv. Mater.* **1998**, *10*, 237.